

Pillar Design Issues for Underground Stone Mines

A. T. Iannacchione, Deputy Director
National Institute for Occupational Safety and Health
Pittsburgh Research Laboratory
Pittsburgh, PA

ABSTRACT

Underground stone mining represents an emerging sector for the U.S. mining industry. As this expansion takes mines under deeper cover and as more efficient mining methods are utilized, adequate stone pillar design methods will become more important. It is the purpose of this paper to examine current design practices and to discuss issues for safe mine layouts so that a rational first approach towards balancing the demands for increased production can be weighed against increased risk to worker safety from rib instabilities and pillar failures. Seventy-two stone mine pillar designs were examined. Pillars with width-to-height ratios below 1.5 and subjected to excessive stress levels appear more likely to fail. When width-to-height ratios fall below 1.0, defects in the pillars, such as through-going discontinuities, can have a significant influence on stability. Discontinuity persistence, dip, material properties, and orientation are important factors controlling pillar strength. The influence of discontinuity dip, a characteristic easily identified in the field, was examined so that its presence could be accounted for in developing generalized guidelines for pillar design.

INTRODUCTION

During the last three years the number of active underground stone mines in the U.S. has ranged between 90 and 100. This number is expected to increase as the crushed stone industry responds to growing demands for their products (Anon, 1998). Additionally, production at underground stone mines is expected to increase above its current level of approximately 66 million metric tons (60 m.st) per year as more of the industry moves towards the unique advantages of underground mining. Parker (1996) identified three advantages for underground operations: 1) surface developments, zoning laws, and environmental concerns are often less of an issue, 2)

stripping and restoration requirements are eliminated, and 3) additional reserves are often available beneath the quarry floor, under pit slopes, or under adjoining property. There are also the added benefits of: 1) working in a constant underground climate rather than the variable surface climate, 2) minimizing community concerns by placing the crushing, sizing, and stowing operations underground, and 3) reducing surface vibration concerns with smaller blast sizes. Drawbacks of underground mining relate to the added health and safety hazards for the stone miners associated with; increased exposure to falls of ground, airborne contaminants, and fog in large underground openings. Also, injuries from falls of ground have occasionally been above incident rates for other mineral resources mined underground (Iannacchione, et al., 1995).

It is clear that existing underground stone operations mine more stone at a faster rate and with larger equipment. Because of high demand there is increasing pressure to yield more stone per production blast. A large majority of the industry uses the V-cut blasting pattern, that limits the magnitude of depth or pull for each shot to about 4 m (13 ft). Therefore, to produce more stone the miners must work more faces or existing faces must be enlarged.

Enlarging underground openings poses problems for maintaining strata stability. First, widths of the mine entries partially control the amount of sag or deflection any given roof beam can withstand before failure. This deflection is, in general, very small and can take place quickly after an opening is excavated or much later as weathering processes aid in forming new, thinner beams. Because increasing deflection increases the potential for roof beam failure, there is some limit to safely widening rooms and these limits depend on local geologic and stress conditions.

Room width limitations have placed more attention on expanding production through benching. Heights of

rooms partially control the strength characteristics of adjacent pillars. As the room height increases for a given pillar width, the pillar width-to-height ratio (w/h) decreases. In general, stone pillars are extremely strong, however, when the width-to-height ratio falls, the potential for pillar rib instabilities and pillar failures increases (Figure 1).

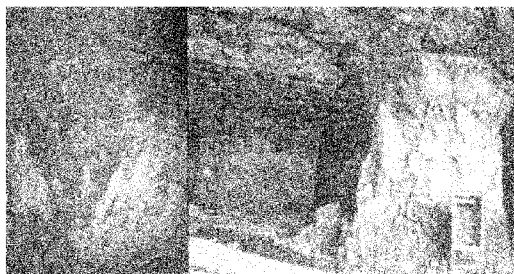


Figure 1 - Photographs of failing pillars. Photo on left shows a crushed edge with a concave shape and photo on right shows a failed pillar in the foreground [Note the crushed ribs and the slender appearance, $w/h < 1$ while the pillar in the background is stable with a $w/h > 1$].

In this environment the desire to utilize wider rooms, higher benches, and multilevel mining may result in the potential for more unstable ground conditions. While the number of failed pillars is currently very low, the potential for additional failures will grow if more slender pillars are developed: 1) especially under deeper cover, 2) with wider mining sections, and 3) in multilevel mining scenarios. It should also be noted that time acts to decrease the strength of many existing pillars. It is the purpose of this paper to examine current design practices and to discuss issues for safe mine layouts so that a rational first approach towards balancing the demands for increased production can be weighed against increased risk to worker safety from rib instabilities and pillar failures.

CURRENT STONE PILLAR DESIGN PRACTICES

The National Institute for Occupational Safety and Health (NIOSH) surveyed 70 underground stone mines to collect information on pillar design practices. Every mine (with one exception) used the room-and-pillar mining method; however, this method has many variations in practice:

- When used in relatively flat lying seams, the pillars are often arranged in regular, reoccurring patterns. Based on the 70 mines surveyed, 93% are regular.
- Occasionally random patterns have been used, although this practice is decreasing in response to improvements in surveying and mine planning. Currently only two mines use the random method.
- The majority of mines use square pillars where the

width of the pillars are equal to the length of the pillars. Nine mines use rectangular pillars (herein referred to as rib pillars) where the pillar length is greater than the pillar width. This design technique has been championed by two prominent consultants in the field, Jim Scott (Iannacchione, 1997) and Jack Parker (1973).

- The room-and-pillar method takes on some unique characteristics when mining steeply dipping beds with multi-levels. Generally, one to three entries are driven along the strike of the strata which may dip from 45 to 70 degrees. Crosscuts are developed horizontally, perpendicular to the entries. Raises or windows between the outer, up-dip crosscuts and the inner, down-dip crosscuts provide for ventilation passages between mining levels. Only 2 mines used this method.
- Finally, the stoping method which employs raises, crown pillars, etc. is used by only one mine.

Because 93% of the mines surveyed uses the regular room-and-pillar technique in a flat lying seam, this paper will focus on analyzing this design method.

In the room-and-pillar mining method, entries and crosscuts are generally driven perpendicular to each other. When these headings are developed horizontally into unmined strata they are called development entries which outline development pillars. Faces are advanced by drilling horizontal holes and blasting the rock back into the development headings. Seventy-two development mining scenarios (two of the 70 mines surveyed used multiple development designs) with 63

Table 1 - Mine layout characteristics for underground U.S. stone mines.

Characteristic		Mean	Standard deviation	Median	Minimum	Maximum
Development	Pillar height, m(ft)	7 (23)	1.7 (5.6)	7 (23)	3.7 (12)	12.2 (40)
	Opening width, m(ft)	13.1 (43)	2.6 (8.6)	12.8 (42)	6.1 (20)	18.3 (60)
	Pillar width, m (ft)	12.2 (40)	4.1 (13.3)	12.2(40)	4.6 (15)	27.4 (90)
	Extraction ratio	0.76	0.07	0.75	0.56	0.91
	Pillar w/h	1.73	0.48	1.72	0.54	3.13
	Overburden, m(ft)	80 (262)	98 (321)	46 (150)	7 (23)	610 (2000)
Bench	Pillar height, m(ft)	14.6 (48)	3.8 (12.5)	14.6 (48)	6.7 (22)	24.4 (80)
	Opening width, m(ft)	13.7 (45)	2.1 (6.9)	13.7 (45)	9.1 (30)	18.3 (60)
	Pillar width, m(ft)	13.1 (43)	4.1 (13.3)	13.7 (45)	6.1 (20)	27.4 (90)
	Pillar w/h	0.92	0.35	0.90	0.4	1.92

square pillar designs and 9 rib pillar designs were examined. Development pillar sizes averaged 12.2 m (40 ft) wide by 7 m (23 ft) high (Table 1). Adjacent rooms averaged 13.1 m (43 ft) in width.

If the stone deposit is thick enough, benching of the floor often occurs. Bench faces are advanced by drilling vertical floor holes from development entries and blasting the rock back into the benched headings. Bench depths average 7.6 m (25 ft). A few of the deeper benches are mined in multiple lifts. Benching does not alter either the widths of the entries or the pillars. It does have an influence on the height of the rooms and pillars, which directly impacts the pillar width-to-height ratio (Table 1). Thirty-five mines bench with the room-and-pillar method.

The distribution of width-to-height ratios for all of the 70 mines surveyed in this study is shown in Figure 2. Two distinct distributions exist based upon the functional characteristics of the pillar. The average pillar width-to-height ratio for development pillars was 1.73 with a standard deviation of 0.48, while the average width-to-height ratio for benched pillars was 0.92 with a standard deviation of 0.35. The distribution of the 72 development pillar designs is somewhat normal while the distribution of the 35 benched pillars is somewhat skewed to the left (Figure 2).

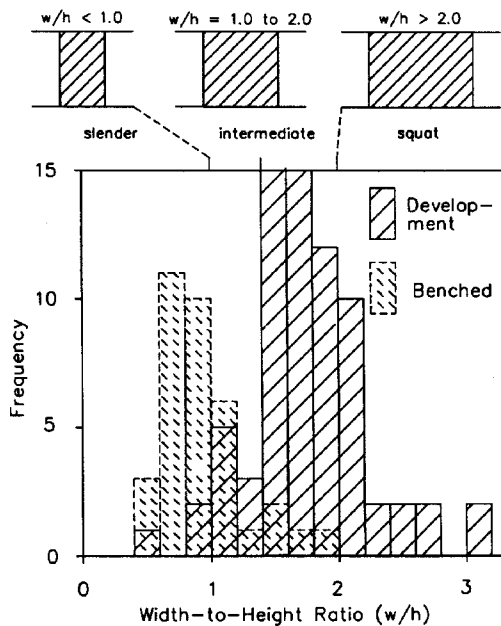


Figure 2 - Width-to-height ratios of pillars used in development and benching sections.

PILLAR PERFORMANCE ISSUES

The extraction ratio is another geometric characteristic which analyzes the relationship between the area of a pillar and the area of the adjacent opening along the horizontal plane. The extraction ratio for perpendicular intersections is determined by the following relationship:

$$e = \frac{(w + r) \times (l + r) - w \times l}{(w + r) \times (l + r)}$$

where
 e = extraction ratio
 w = pillar width
 l = pillar length
 r = opening width

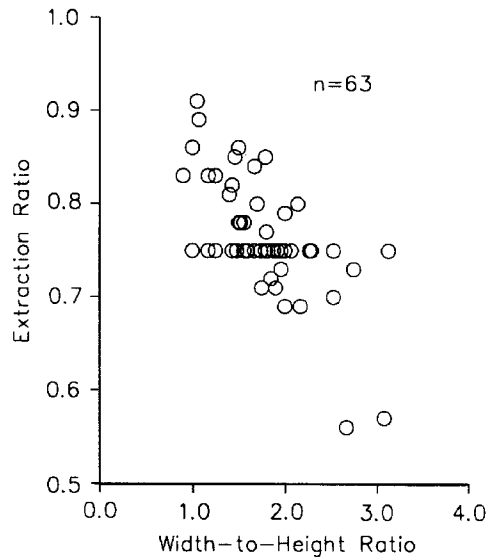


Figure 3 - Comparison between square pillar width-to-height ratios and the extraction ratios for development mining.

Figure 3 shows the relationship between the extraction ratio for square development rooms-and-pillars and the width-to-height ratios for these same pillars. In general, the extraction ratio decreases as the width-to-height ratio increases. This is expected because both ratios consider the pillar width as a factor. The safety concern is that as the extraction ratio increases the pillars receive higher levels of stress, while these pillars in a sense are becoming more slender. Obviously, slender pillars are inherently less stable.

Depending on the years of mining, an underground stone mine may have a few dozen to several thousand pillars. The vast majority of these pillars are adequately

sized and currently stable. However, pillar design is seldom explicitly addressed. Pillar stability should be more closely examined under: 1) excessive stress levels, 2) adverse geologic conditions, and 3) increasing time.

Stress Levels

Generally, stone pillars are less stable if overburden is substantial because of the higher stress. Pillars are also less stable as the width-to-height ratio decreases such as in benching operations. Stress levels within pillars can be approximated by using the tributary area theory (Brady and Brown, 1985):

$$\sigma_a = \sigma_o \times \frac{(r + w) \times (r + l)}{w \times l}$$

where: σ_a = average post mining vertical stress
 σ_o = premining vertical stress

Pillar stress levels are affected by the overburden and the relationship between the area supported by the pillar and the area of the pillar. This relationship is illustrated by comparing the post mining vertical stress levels as the overburden and the extraction ratio increase. Figure 4 shows the relationship between average pillar stress, overburden, and extraction ratio for a 13.7 m (45ft) wide opening with square pillars. As overburden and extraction ratios increase, the stress levels rise exponentially. Incremental changes in overburden result in a proportional change in the average pillar stress levels at specific extraction ratios. Increasing extraction ratios produce an exponential rise in the average pillar stress levels at specific overburdens. At most underground stone mines, overburden averages 80 m

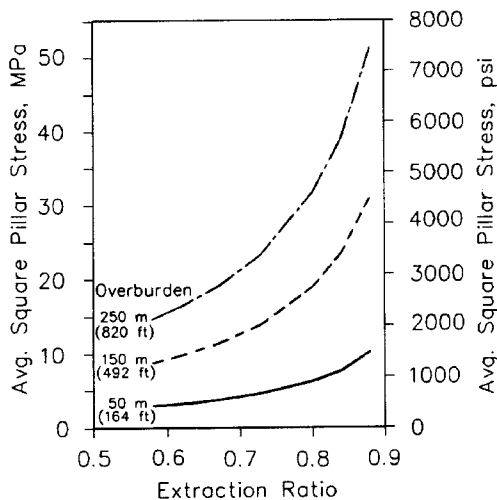


Figure 4 - Relationship between average pillar stress levels, extraction ratio, and overburden for a 13.7 m (45 ft) wide opening with square pillars.

(262 ft), thus excessive stress levels would not be expected to result in pillar failure. The relatively shallow depth of most underground stone mines is why pillar shape and size are often overlooked as a safety issue during mine design and development.

Pillar Strength

The most generally accepted techniques for determining pillar strength, defined as the ultimate load per unit area of a pillar, use empirical derivations based on survey data from actual mining conditions. The power of the empirical method is that specific failure mechanism need not be considered. The failings of the method stems from an inability to extend these formulae beyond the specific material properties, sizes, shapes, and overburdens found in the survey data. Bieniawski (1984) wrote that the strength of mine pillars is dependent upon three elements: 1) the size or volume effect (strength reduction from a small laboratory specimen of rock to full size mine pillars); 2) the effect of pillar geometry (shape effect); and 3) the properties of the pillar material. For non-coal pillars, empirical formulas have largely been derived from some form of the following power formula:

$$\sigma_p = \sigma_m \times \frac{w^a}{h^b}$$

where σ_p = Pillar strength (ultimate)
 σ_m = Material strength
 h = pillar height
 a, b = constants derived from laboratory or field experiments

This formulation considers both material strength and pillar shape to calculate pillar strength.

Material Strength: In these equations, the material strength (σ_m) of a nominal size pillar is generally approximated by reducing the uniaxial compressive strength (σ_c) of the material from laboratory testing of small cylindrical or cubed shaped specimens. Laboratory test samples typically over-estimate rock material strength values because larger flaws or fractures are exhibited as specimen size increases. At some point specimen size becomes large enough so that further reductions in material strength become insignificant. This is often referred to as rock mass strength. Bieniawski (1984) suggested that cubic coal specimens from 0.9 to 1.5 m (3 to 5 ft) are of a critical size and are representative of rock mass characteristics. Hedley and Grant (1972) used an equivalent material strength value representative of a 0.3 m (1 ft) cube of quartzite. Others have used reduction factors ranging from 40 to 80 % to determine material strength from uniaxial compressive strength values.

Pillar Shape: Several pillar strength equations have been expressed as a power function of the pillar's height and width. Salamon and Munro (1967) derived the following equation after analyzing 125 case studies from South African coal mines:

$$\sigma_p = 1320 \times \frac{w^{0.46}}{h^{0.66}}, (\text{psi})$$

In this equation a material strength (σ_m) equivalent to 9.1 Mpa (1320 psi) was used because coal has a relatively low material strength compared to most industrial minerals and metal mine rocks. Hedley and Grant (1972) extended this power function to describe the strength of quartzite pillars in deep uranium mines near Elliot Lake, Canada:

$$\sigma_p = 26000 \times \frac{w^{0.5}}{h^{0.75}}, (\text{psi})$$

The equation is similar to Salamon and Monroe with the exception of a higher material strength value for the stiff uranium host rock. In this case the material strength of uranium pillars is close to 20 times greater than for South African coal. An alternative application of a pillar strength formula was suggested by Hardy and Agapito (1975). From a study of oil shale pillars in western Colorado, the appropriate pillar strength formula was inferred to be of the form:

$$\sigma_p = \sigma_c \times \left(\frac{v_p}{v_s} \right)^{-0.118} \times \left(\frac{w_p}{h_p} / \frac{w_s}{h_s} \right)^{0.833}$$

Where: σ_c = Uniaxial compressive strength of sample
 v = Volume of pillar/sample

This method involves determining the uniaxial compressive strength of a specimen where subscripts p and s refer to pillar and specimen, respectively.

Power functions produce a very distinctive relationship between strength and width-to-height ratio (Figure 5). At low width-to-height ratios (< 1.0), pillar strength rises rapidly. At higher width-to-height ratios strength increases occur at diminishing rates. In other words, at some point the pillar would begin to display some plastic behavior. Barron referred to this as pseudo-ductile behavior (Barron, 1984). The occurrence of pseudo-ductility in coal pillars has been debated for years. It seems unlikely that stiff, brittle materials like stone or other hard rocks would display this same type of plastic behavior. In fact, there has been a recognition that at width-to-height ratios greater than 4 or 5, strain hardening behavior can occur (Salamon and Wagner, 1985, Stacey and Page, 1986).

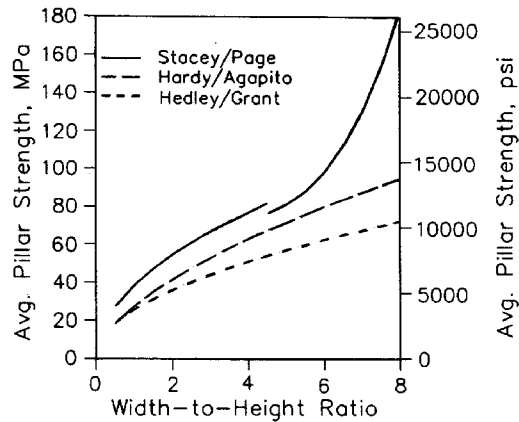


Figure 5 - Comparison between pillar width-to-height ratio and average pillar strength for several different empirical equations based on a power function. Note: material strength was normalized for each equation for comparative purposes.

The approach suggested by Stacey and Page (1986) takes this behavior into account by producing exponential rises in pillar strength at higher width-to-height ratios:

for $w/h < 4.5$

$$\sigma_p = k \times \frac{w^{0.5}}{h^{0.7}}, (\text{MPa})$$

for $w/h > 4.5$

$$\sigma_p = k \times \frac{2.5}{\sqrt{0.07}} \times \left(0.13 \times \left[\left(\frac{w_{\text{eff}}}{h} \right)^{4.5} - 1 \right] + 1 \right), (\text{MPa})$$

Where: $k = \sigma_m \times \text{DRMS}$ (Design Rock Mass Strength)
 $\text{DRMS} = \sigma_c$ adjustment factor (Stacey and Page, 1986)
 $V = w_{\text{eff}}^2 \times h$
 $w_{\text{eff}} = 4 \times A_p / R$
 A_p = plan area of the pillar
 R = perimeter

Here the pillar strength follows a power function for relatively low width-to-height ratio (< 4.5) and then begins to follow an exponential rise above width-to-height ratio > 4.5 (Figure 5).

The application of these formula to underground stone is problematic. It seems unlikely that increasing the pillar width-to-height ratio would result in a gradual

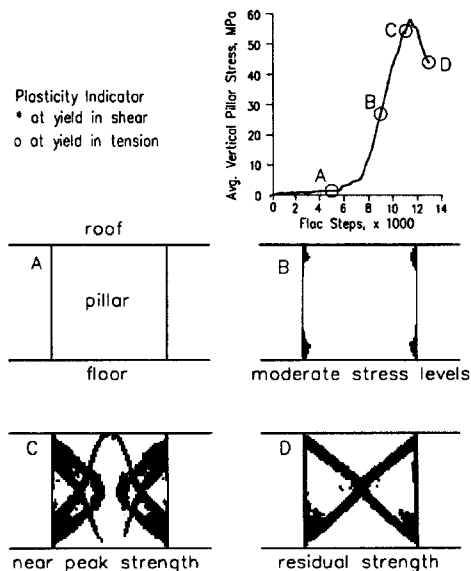


Figure 6 - An elastic-plastic model, which produces progressive failure patterns, can exhibit strain-softening behavior within full scale pillars.

decrease in the rise in pillar strength. In fact, in practice just the opposite appears to occur. Pillar stability is most endangered at low width-to-height ratios. As typical stone pillars reach a width-to-height ratio >1.5 , they begin to exhibit an almost indestructible character. The Stacey and Page (1986) formula appears to accommodate both the traditional strength flattening at moderate width-to-height ratios (~ 4 to 5) as proposed by Salamon and Munroe (1967) and the exponential rise in pillar strength at high width-to-height ratios. Unfortunately this strength adjustment occurs at width-to-height ratios that are well outside the ranges of all stone mines surveyed.

STONE PILLAR BEHAVIOR - Progressive Failure

The above techniques do not provide a totally realistic picture of stone pillar behavior. Additionally, a large database of pillar specific information of past successes and failures hasn't been established to aid in constructing a reliable pillar design technique for stone mines. In the absence of this information, numerical simulations can produce a potentially useful means to test engineering methods. The simulation used for this study was the 2 and 3-dimensional finite difference code (ANON, 1998). The 2-dimensional calculations were performed under plane-strain conditions, so the model sample is equivalent to a long pillar. It is assumed that individual elements in the model behave in an elastic-perfectly plastic behavior, however, the overall pillar

behavior can include strain-softening and strain-hardening. Model shapes mirrored those observed in the field ranging from a very slender pillar with a width-to-height ratio of 0.4 through intermediate pillars with a width-to-height ratio of 1.4. With slender shapes, pillars failed rapidly by yielding from the ribs inward to the pillar core, indicating a relatively low strength structure. As pillars become more squat, elevated horizontal confinement dramatically increases pillar strength. Model symmetry was constructed so as to simulate a reoccurring pattern of rooms and pillars of equal dimensions. The roof and floor material were modeled to be elastic.

The model pillars had a moduli of 41.4 GPa (6,000,000 psi), an angle of internal friction of 40° , and a cohesion of 6.9 MPa (1,000 psi). The model pillars were subjected to simulated loading conditions by moving distant boundaries in the roof and floor together at very slow rates. This had the effect of gradually loading the pillars through several distinct strength phases. During the early loading phase the modeled pillar displays relatively elastic characteristics (Figure 6, Points A to B), where the pillar deformation is proportional to increases in average vertical stress levels within the pillar.

During this phase dominated by elastic behavior, minor yielding of the pillar edges begins to occur. Continued progressive failure of the pillar's outer perimeter produces an hour-glass shaped elastic core. It also has the effect of moving the peak vertical stress away from the pillar edge and toward the pillar center (Figure 6, Points B to C).

The maximum pillar strength was achieved when the highest vertical stress levels in the elastic core were supported by the maximum horizontal confinement available to the pillar (Figure 6, Point C). Beyond this point, any additional load to the pillar resulted in a rapid loss of strength. The zone of plastic yield extended throughout the pillar producing a residual pillar strength (Figure 6, Point D) which was considerably less than the maximum pillar strength.

THE EFFECT OF EXCESSIVE STRESS ON STONE PILLAR STABILITY

Pillar failure due to excessive stress levels was not frequently observed during field visits to underground stone mines. In fact, there were only seven development pillars at four mines that were observed to have undergone progressive failure due to excessive loading (Table 2). In Case 1 (Table 2) a pillar with a width-to-height ratio of 1.0 was inadvertently reduced from 9.1 to 6.1 m (30 to 20 ft) under less than 30 m (100 ft) of overburden. This pillar had an average vertical stress of less than 7 MPa (1000 psi). Failure of the pillar perimeter due to crushing left only a narrow core of

broken rock (photo on right, Figure 1). It was surmised that additional stresses were applied to the pillar either as a result of its unique position near the highwall or due to some undetected geologic characteristic.

In Case 2, the initial mine development had occurred with random room-and-pillar methods. One failed pillar was observed that was narrower than the surrounding pillars. This pillar had a width-to-height ratio of 1.25 while adjacent pillars were in excess of 2.0. Here again it was difficult to determine what level of stresses caused failure since the overburden was very low.

Table 2 - Characteristics of development pillars that failed

Case	Observed failed pillars	Pillar width, m (ft)	Pillar height, m (ft)	w/h ratio	extraction ratio	Remark
1	1	6.1 (20)	6.1 (20)	1.0	0.94	Reduced pillar size
2	1	6.1 (20)	4.9 (16)	1.25	0.92	Smallest pillar in a non-regular mining area
3	1	5.5 (18)	6.1 (20)	0.9	0.86	High overburden stress and reduced pillar size
4	4	3 to 6.1 (10 to 20)	7.3 (24)	0.42 to 0.83	0.9 to 0.83	High overburden stress

In Case 3, a pillar with a width-to-height ratio of 0.9 was inadvertently reduced from 9.1 to 6.1 m (30 to 20 ft) under a high overburden condition of approximately 275 m (900 ft). Average vertical stresses on this pillar could have exceeded 28 MPa (4000 psi). The failed pillars had shear surfaces that began and terminated at the pillar-roof and pillar-floor intersections and propagated inward in a convex shape (photo on left, Figure 1).

In Case 4, the overburden ranged from 230 to 260 m (750 to 850 ft), producing an average vertical stress that was generally less than 14 MPa (2000 psi) on pillars with openings that ranged between 15 to 18 m (50 and 60 ft) in width and width-to-height ratios that averaged 2.1. In several areas within this large mine, pillars of reduced width with width-to-height ratios ranging from 0.83 to 0.42 were subjected to average vertical stresses that could have reached 35 MPa (5000 psi). At least four of these pillars exhibited a very distinctive concave failure surface that resembled an "onion skin". As the failure process continued, the pillar size was reduced, thereby increasing the extraction ratio and resulting in higher stress and more pillar deterioration.

As underground stone production expands, mining depths (overburden) are expected to increase. Presently six mines in the Valley and Ridge Province of Pennsylvania, Virginia, and Tennessee and two mines in Kentucky are mining at depths between 250 to 600 m (800 to 2000 ft). Many more mines will soon be

encountering their first 100 to 150 m (330 to 500 ft) overburdens. As depth of mining increases the potential for excessive stress levels that adversely affect pillar stability will also increase substantially.

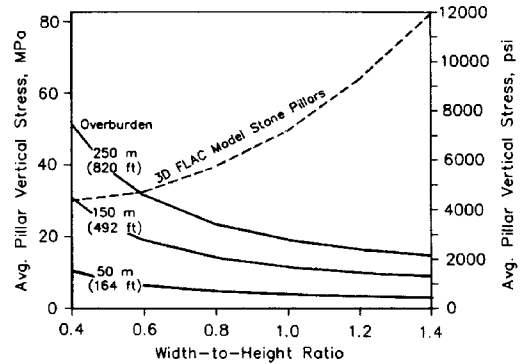


Figure 7 - Changes in stone pillar strength at width-to-height ratios ranging from 0.4 to 1.4.

In the absence of specific design information for underground stone mines, the following pillar design guidelines related to excessive stress levels are proposed. These guidelines consider the previous numerical simulations as a means of examining how pillars of various shapes will be affected under different overburdens. Figure 7 shows the changes in average vertical stress conditions at different overburdens and different width-to-height ratios using the tributary area theory. The solid black line represents the strength of a modeled pillar, free of discontinuities, as its shape changes from a slender pillar (w/h=0.4) to an intermediate pillar (w/h=1.4). This modeled pillar has a stiffness of 41.4 GPa (6 million psi) and a failure envelope defined by a friction angle (ϕ) of 40° and a cohesion of 6.9 MPa (1000 psi). These values represent typical material strength characteristics of Loyalhanna Limestone of Pennsylvania and West Virginia.

In this example, our model pillar with a width-to-height ratio of 1.4 could potentially accommodate an average vertical stress of approximately 80 MPa (12000 psi). Clearly a pillar of this strength, free of discontinuities, could withstand all of the extraction ratio and overburden conditions shown in Figure 4. Conversely a slender pillar, with a width-to-height ratio of 0.6 and 250 m (820 ft) of overburden, might fail. Note that the FLAC model strength curve has a shape very different from those curves determined by the empirical design techniques illustrated in Figure 5. At low width-to-height ratios pillars are low in strength. As width-to-height ratios increase to 1.0 and beyond, the pillar strength increases considerably. At a width-to-height ratio of greater than 1.5, pillars free of geologic discontinuities are unlikely to fail. The shape of the pillar strength curve shown in Figure 7 is defined by the stiffness of the material and shape of the failure

envelope, which is defined by the friction angle and the material cohesion used in the model.

THE EFFECT OF DISCONTINUITIES ON STONE PILLAR STABILITY

The stability of a stone pillar is highly influenced by overburden stresses and the occurrence of geologic discontinuities. Observations of pillar conditions have shown that the presence of geologic discontinuities represents a more likely potential safety concern for mine workers than excessive stress levels. When a room is heightened, the area of the rib increases, which elevates the potential for exposure of geologic discontinuities and mining induced damage intersecting the rib. Characteristics of geologic discontinuities, such as bedding planes, slips, faults, and joints, include frequencies, persistence, straightness, strike, dip, and material properties. Mining induced damage can result from drilling, blasting, or scaling operations, and is an extremely important factor in designing safe, stable pillars, but is not considered in this report.

Bench Mining Case Studies

The best way to analyze the influence of geologic discontinuities on pillar stability is to evaluate the pillar performance in benching operations where pillar shapes are generally slender. A comparison of pillar shape, room width, and pillar height of 35 square bench pillar designs is shown in Figure 8. There appears to be no clear correlation between pillar height or room width and

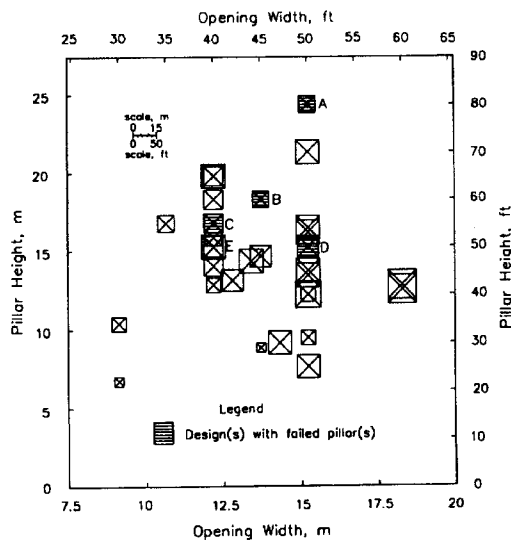


Figure 8. - Comparison of pillar shape, opening width, and pillar height of 35 square bench pillar designs. Note that changes in square size are proportional to changes in pillar sizes.

pillar failure. Indeed, three of the four designs with some failed pillars had only moderate pillar widths and heights (Figure 8, Points B, C, and D). These operations were all mining in a formation which is known to have a higher than normal occurrence of large, angular geologic discontinuities. The fourth design with failed pillars (Figure 8, Point A) was used in a formation not known to have a high occurrence of geologic discontinuities. Here pillar failure was probably associated with the slenderness of the pillar ($w/h=0.5$).

There are several factors that make the character of the geologic discontinuity significant:

- Persistence - the length of the discontinuity must be on the same scale as the pillar it is effecting if strength is to be impacted,
- Dip - the dip of the discontinuity can dramatically affects pillar strength (Figure 9),
- Frequency - the spacing between discontinuities is very important in determining the potential for failure in a large mining area,
- Material Properties - the properties of the discontinuity can be used to assess the magnitude of strength reduction, and
- Orientation - the orientation of the discontinuity is important when the pillars are rectangular, in that, strength will be most affected when the orientation of the discontinuity is aligned with the long axis of the pillar.

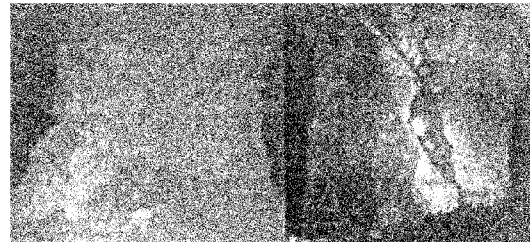


Figure 9 - The left pillar has a discontinuity dipping at approximately 20° while the right pillar's discontinuity dips at approximately 60°.

Characteristics of Discontinuities

Several of these factors can be considered by utilizing the analytical procedure discussed by Farmer (1983):

$$\sigma_1 = \frac{2C_d + 2\sigma_3 \tan \phi_d}{(1 - \cot \beta \tan \phi_d) \sin 2\beta}$$

where

σ_1 = Vertical strength,

σ_3 = Confinement,

C_d = Cohesion along the discontinuity,

ϕ_d = Friction angle along the discontinuity, and

β = Dip of discontinuity measured from the vertical axis.

Figure 10 shows how sample strength varies for different discontinuity dip angles under a range of discontinuity material properties. This analysis is instructive in demonstrating the relative magnitude of strength reduction based on discontinuity dip angle. It also shows how friction angle and cohesion along the discontinuity individually affect unit strength. However, this technique can have limited value in analyzing stone pillar behavior with discontinuities because it treats the material as one uniform elastic mass.

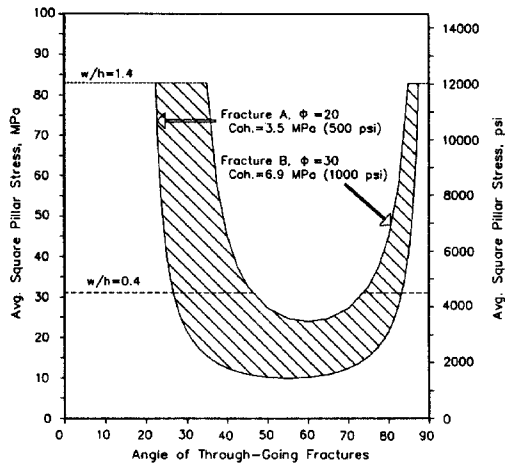


Figure 10 - The affect of angular geologic discontinuities on vertical strength using an analytical technique.

An alternative approach is to introduce simulated discontinuities into the previously discussed finite difference elastic-plastic pillar model and rotate the interface through a series of angles. In this way variations in material properties, discontinuity dips, and pillar shapes can be evaluated. This was accomplished by utilizing the ubiquitous joint model in the FLAC 3D program. The ubiquitous-joint model is an anisotropic plasticity model that includes weak planes of specific orientation embedded in a Mohr-Coulomb solid. In this model, yield may occur in either the intact rock or along a joint (discontinuity), or both, depending on the stress state, the orientation of the joint plane, and the material properties of the intact rock and joint plane.

Parametric analysis of the effect of discontinuities on pillar strength was conducted by varying the dip and material properties within the ubiquitous joint model. These simulations passed discontinuities through modeled pillar shapes that ranged from width-to-height ratios of 0.6 to 1.2. Three distinct pillar behaviors were observed based on the dip of the discontinuities. Figure 11 shows the strength profiles for pillars with a stiffness of 41.4 GPa (6 million psi) and a Mohr-Coulomb failure envelope defined by a friction angle of 40° and a discontinuity friction angle of 25°. The lowest pillar

strength occurred at a discontinuity dip angle of 57.5° (Figure 11). It should be noted that the point of lowest strength is defined in the ubiquitous joint model by the following relationship:

$$\beta_{\min} = 45 + \frac{\phi_d}{2}$$

where:

β_{\min} = Angle of through-going discontinuity which produces the lowest average vertical peak stress,
 ϕ_d = Internal angle of friction for the discontinuity.

How well this model characteristic fits field conditions needs to be evaluated further. The highest pillar strength occurred with a discontinuity dip of 0° and gradually decreased as discontinuity dip angle increased. As the discontinuity dip angle increased above 57.5°, pillar strength began to increase again; however, the original strength for the intermediate to squat pillar shapes was not reestablished.

For all model shapes, and for a given set of material properties, pillar strength associated with the discontinuity dip of 90° was the same. In the case of the example shown in Figure 11 that value was approximately 29 MPa (4200 psi). It should be noted that this characteristic may be model driven and not representative of field conditions. The ubiquitous joint model would attempt to force discontinuities through columns of equally sized grid elements. While this behavior may be indicative of successive column failure through a pillar with numerous equally spaced vertical joints, it may not be indicative of pillars affected by variably spaced joints.

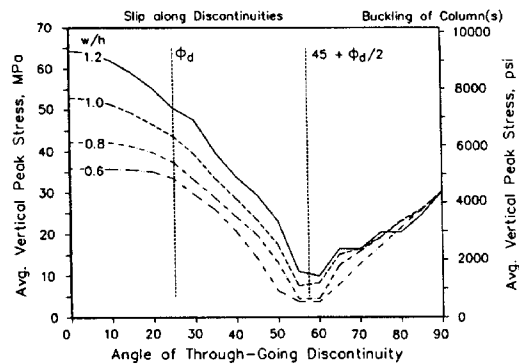


Figure 11 - Changes in average vertical peak stress as discontinuity dips are varied from 0 to 90° for four different width-to-height ratio model pillars.

Stress versus strain plots for these numerical simulations are shown in Figure 12. For discontinuity dips between 0 and 45° the material displayed an elastic-plastic behavior. When this models was run with

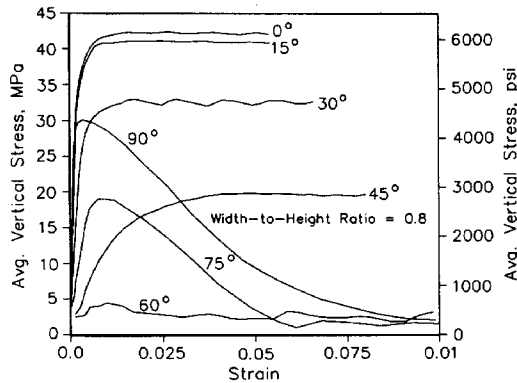


Figure 12 - Stress versus strain for model pillars (width-to-height ratio = 0.8) with discontinuity dips ranging from 0 to 90°.

a discontinuity dips of 60°, the model pillar exhibited very low strength. Finally, strain softening material behavior occurred as discontinuity dips increased to 90°. The conclusion of this effort is that both observation and numerical data suggest that when discontinuities are present at a particular angle and composition, they can control the behavior and strength of pillars.

The impact of this analysis is detailed in Figure 13. The strength of pillars with various shapes and different discontinuity dips are very sensitive to changes in extraction ratio and overburden. For example, a discontinuity dipping at 60°, under approximately 50 m (165 ft) of overburden, with a width-to-height ratio of 0.8, and passing through the entire 15 m (50 ft) high pillar, could fail if its properties were equivalent to material with a friction angle of 25° and a cohesion of zero. If this same discontinuity dips at 45°, the pillar might not fail until almost 250 m (820 ft) of overburden is encountered. Figure 13 is presented to illustrate the significant impact that pillar shape, overburden, and discontinuities can have on stone pillar strength and is not meant to be a design guideline.

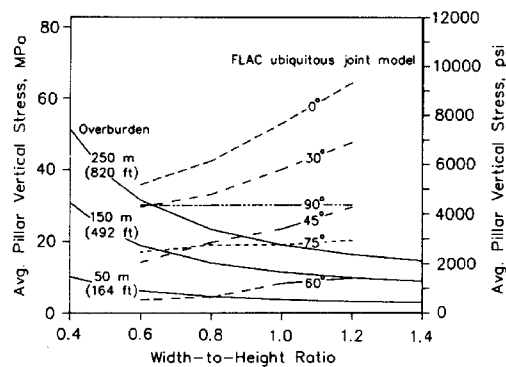


Figure 13 - Relationship between pillar shape, overburden, discontinuity dip and pillar strength.

SUMMARY AND CONCLUSIONS

The intent of this report is to create an awareness in relation to mine worker safety of the potential for pillar failure, particularly in operations that bench. As underground stone mining expands and depth of overburden increases, consideration of the appropriate size and shape of pillars should be an integral part of the overall mine design. Using data gathered from in mine visits, mine maps, discussions with operators, and numerical simulations, stone pillar design issues were investigated and general guidelines were discussed. The important pillar design issues and guidelines can be summarized as follows:

- Most stone pillar have relatively low width-to-height ratios, ranging from 0.54 to 3.13, and high extraction ratios, ranging from 0.56 to 0.91. This results in many pillars having shapes that are slender with relatively large adjacent mine openings.
- Excessive vertical stress levels are generally not a serious problem in stone mines because the pillar material is often very strong and the overburdens are typically very low (average overburden = 80 m [262 ft]). However, there are a few known cases where pillars have failed due to excessive stress levels. These cases were associated with local unintentional pillar size reduction, overburdens greater than 200 m (630 ft), width-to-height ratios less than 1.25, or extraction ratios greater than 0.83. As depth of mining increases, the potential for excessive stress levels that adversely affect pillar stability will also increase substantially.
- The strength of slender pillars is best understood by examining models which allow for shape variations and progressive failure through elastic-plastic or strain softening behavior. Models which met this criteria were examined in the paper and demonstrated that stone pillar strength should not follow a linear relationship with pillar shape. Empirical strength formulas for metal/nonmetal mines produce power curves which produce higher pillar strengths at low width-to-height ratios (<1.0) and lower pillar strengths at moderate to high width-to-height ratios (>1.5).
- Bench mining produces slender pillars. Where geologic discontinuities are present, the potential for pillar failures increases. The persistence, dip, frequency, and material properties of these discontinuities control pillar strength.
- A strong correlation was found between the material properties and dip of discontinuity and the modeled pillar strength. As discontinuity dips increased from 0 to $45 + \phi_d/2$, pillar strength gradually decreased. When the dips were equal to $45 + \phi_d/2$, pillars exhibited a very unstable behavior, losing considerable levels of their original strength. As vertical orientations were approached, columns defined by discontinuities can control pillar behavior.

The pillar design guidelines developed through the observational and numerical simulations discussed above will require further field confirmation. This information has been presented so that mine planners, operators, and workers can recognize the potential hazards that exist when designing stone pillars. This approach can help to form a part of a comprehensive pro-active mine safety ground control plan for underground stone mines.

REFERENCES

- Anon, "Highway-Building Surge", Wall Street Journal, June 2, 1998, PP, pA1(W)-pA1(E).
- Anon, "FLAC: Fast Lagrangian Analysis of Continua User's Guide", Itasca Consulting Group, Inc., Minneapolis, MN, 1998.
- Barron, K., "An Analytical Approach to the Design of Coal Pillars, CIM Bull., Vol. 77, No. 868, Aug. 1984, pp. 37-44.
- Bieniawski, Z.T., Rock Mechanics Design in Mining and Tunneling, Balkema, Rotterdam, 1984, pp. 193-209.
- Brady, B.H.G. and E.T. Brown, "Rock Mechanics for Underground Mining", George Allen and Unwin, London, 1985, pp. 320-325.
- Farmer, I.W., Engineering Behaviour of Rocks, Chapman and Hill, London, 1983, pp. 151-158.
- Hardy, M.P. and J.F.T. Agapito, "Pillar Design in Underground Oil Shale Mines", In Design Methods in Rock Mechanics, Proc. 16th Symp. on Rock Mechanics, C Fairhurst and S.L. Crouch (ed), Minneapolis, MN, 1975, pp. 257-266.
- Hedley, D.G.F. and F. Grant, "Stope-and-Pillar Design for the Elliot Lake Uranium Mines", CIM Transactions, Vol. 75, 1972, pp. 121-128.
- Iannacchione, A.T., T. P. Mucho, and L. J. Prosser, "Ground Control Problems in the Underground Limestone Industry," Proc. of the Environment, Safety, and Health Forum (National Stone Assoc), Nashville, TN, Oct. 22-24, 1995.
- Iannacchione, A. T. and L. J. Prosser, "Roof and Rib Hazard Assessment for Underground Stone Mines," SME Preprint 97-113, SME Annual Meeting, Denver, CO, Feb. 24-27, 1997, 5 pp.
- Parker, J., "How to Design Better Mine Openings: Practical Rock Mechanics for Miners," Engineering and Mining Journal, Part 5, December 1973, pp. 76-80.
- Parker, J., "Everybody Goes Underground Eventually", Aggregate Manager, June 1996, pp. 30-35.
- Salamon, M.D.G. and A.H. Munro, "A Study of the Strength of Coal Pillars", Journal of the South African Institute of Mining and Metallurgy, Sept. 1967, pp. 55-67.
- Salamon, M.D.G. and H. Wagner, "Practical Experience in the Design of Coal Pillars", Proc. of the 21st Int. Conf. of Safety in Mines Research Institutes, Sydney, Australia, 1985, pp. 3-10.
- Stacey, T.R. and C.H. Page, "Practical Handbook for Underground Rock Mechanics", Series on Rock and Soil Mechanics, Vol. 12, Trans Tech Publications, 1986, pp. 53-63.